This article has been accepted for publication in a future issue of this journal, but has not been fully edited. Content may change prior to final publication. Citation information: DOI 10.1109/TEC.2018.2841427, IEEE Transactions on Energy Conversion

SoH-Aware Charging of Supercapacitors with Energy Efficiency Maximization

Heng Li, *Member, IEEE*, Jun Peng, *Member, IEEE*, Yanhui Zhou, Jianping He, *Member, IEEE*, Zhiwu Huang, *Member, IEEE*, Liang He, *Senior Member, IEEE* and Jianping Pan, *Senior Member, IEEE*

***Abstract*—Recent years have seen significant advances in supercapacitor-based applications in portable electronics, where the switching resistor circuit acts as a common cell balancing circuit when charging the supercapacitors. However, existing charging control methods suffer from low energy efficiency, leading to considerable energy loss and thermal heating. In this paper, we propose a state-of-health (SoH)-aware energy-efficient charging method to maximize the energy efficiency of supercapacitors during the charging process. First, we provide a sufficient and necessary condition to maximize the energy efficiency. Then, an online SoH estimation algorithm is designed to estimate capacitance and balancing resistance in real time. Thereafter, an SoH-aware energy-efficient charging algorithm is further proposed to be implemented in micro-controllers. A charger prototype has been built to verify the effectiveness of the proposed charging algorithm. Extensive simulation and experiment results show that the energy efficiency of the proposed design is improved considerably when compared with existing methods.**

***Index Terms*—Supercapacitors, state-of-health, energy efficiency, charging, portable applications**

I. Introduction

Supercapacitors are traditionally used in high-power applications such as regenerative braking in cars/trains/elevators [1], in complementary to other forms of energy storage such as batteries. Actually, supercapacitors' high power capacity also enables their super fast charging [2] — e.g., the onboard supercapacitor can be fully charged in 30 seconds [3], which has recently expanded their applications to low-power systems such as wearable devices [4], implantable medical devices [5], and portable chargers [6], as the single power source. In these systems, supercapacitor cells are typically connected in series as a module to fulfill the system's voltage requirement [7].

This work is partially supported by Hunan Science and Technology Plan Project, National Natural Science Foundation of China (Grant No. 61672537, 61772558 and 61773257), NSF CNS-1739577, and NSERC of Canada. (*Corresponding Author:* Zhiwu Huang)

Heng Li is with School of Information Science and Engineering, Central South University, Changsha, China, 410083, and also with Department of Computer Science, University of Victoria, Victoria, BC, Canada, V8W3P6 (email: liheng@csu.edu.cn).

Jun Peng, Yanhui Zhou, and Zhiwu Huang are with School of Information Science and Engineering, Central South University, Changsha, China, 410083 (email: hzw@csu.edu.cn).

Jianping He is with Department of Automation, Shanghai Jiao Tong University, and The Key Laboratory of System Control and Information Processing, Ministry of Education of China, Shanghai, China, 200240 (email: jianpinghe.zju@gmail.com).

Liang He is with Department of Computer Science and Engineering, University of Colorado Denver, Denver, Colorado, USA, CO, 80124 (email: liang.he@ucdenver.edu).

Jianping Pan is with Department of Computer Science, University of Victoria, Victoria, BC, Canada, V8W3P6 (email: pan@uvic.ca).

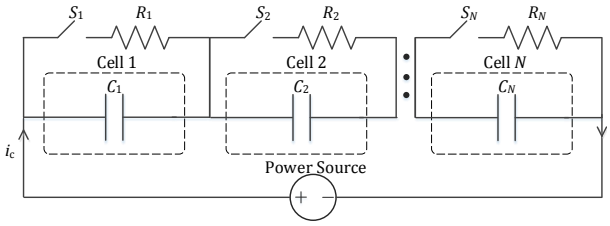

Fig. 1. The switched resistor circuit to balance N cells.

Supercapacitor cells, however, suffer from cell imbalance due to manufacturing limitations and uneven state-of-health (SoH) degradations [8], causing cell overcharging easily when charging the supercapacitor module [9]. As a result, external balancing circuits are used to mitigate the imbalance and protect cells from overcharging. Switched resistor circuit is a widely deployed solution for such cell balancing because of its good trade-off between performance and cost [7], especially for portable applications with the limited system size and cost budget. Fig. 1 illustrates the schematic of the switched resistor circuit, where each cell is connected in parallel with a resistor via a switch.

Different control methods for supercapacitor charging have been proposed in the literature. The classic one is the $1-$ charging method, where the duty cycles of all switches are always 1, i.e., switches are kept on all the time [10]. This charging method simplifies the circuit design but prolongs the charging time [11]. Another classic charging control method is the $0-1$ charging, where switches are on if the corresponding cells are fully charged, and vice versa. The $0-1$ charging method has been widely used in industrial applications [12]. Other advanced control approaches have also been proposed to further improve the charging performance [13], [14]. In [13], a model predictive control strategy is proposed to prolong the lifetime by considering the temperature deviations of the circuit. In [14], an average-consensus based charging control method is proposed to handle the voltage deviations of the $0-1$ method, where control decisions are made based on the voltage comparisons with neighbors.

However, existing charging control methods are not explicitly designed to maximize the energy efficiency, which is crucial for supercapacitors: (i) with the same stored energy in supercapacitors, maximizing energy efficiency implies less consumed energy from the power source, thus rendering the charging system greener; (ii) maximizing energy efficiency means less energy loss, and thus the thermal heating can be

0885-8969 (c) 2018 IEEE. Personal use is permitted, but republication/redistribution requires IEEE permission. See http://www.ieee.org/publications_standards/publications/rights/index.html for more information.

This article has been accepted for publication in a future issue of this journal, but has not been fully edited. Content may change prior to final publication. Citation information: DOI 10.1109/TEC.2018.2841427, IEEE Transactions on Energy Conversion

alleviated and the system reliability can be improved [13].

To close this gap, in this paper, we propose an SoH-aware energy-efficient charging (SoH-aware EFC) method for supercapacitors. This design is steered by an analytically revealed sufficient and necessary condition to maximize the energy efficiency during charging. Implementing this condition in practice, however, requires the real-time knowledge on supercapacitors' SoHs, to which end a recursive-least-square (RLS)-based online SoH estimation method is further proposed.

We have implemented and evaluated the proposed method on a prototyping system. The results show at least 7.5% improvement in energy efficiency when compared with existing methods. Moreover, in cases of severe SoH degradation, SoH-aware EFC improves the energy efficiency by 8.6% and shortens the charging time by 18.4%.

The contributions of this paper are three-fold.

- We analyze why existing charging methods cannot maximize the energy efficiency and suggest its remedy;
- An SoH-aware EFC method is proposed to maximize the charging efficiency of supercapacitor cells;
- The SoH-aware EFC method is evaluated with both simulations and experiments, and the results show its effectiveness and superiority over existing methods.

The remainder of this paper is organized as follows. The related work is introduced in Section II. The preliminaries and motivations are presented in Section III. In Section IV, we introduce the SoH-aware energy-efficient charging method. Simulation and experiment results are provided in Section V. We conclude the paper in Section VI.

II. Related Work

In portable applications, supercapacitor cells are typically embedded in devices, and are usually inaccessible and maintenance-free [5]. During the long-term operation, the aging of cells leads to their SoH degradations, observed as decreased capacitance and increased equivalent-serial-resistance (ESR) [15], making it crucial to monitor supercapacitor parameters in real time.

Online SoH estimation for supercapacitors has received increasing attentions in the past few years [16]–[20]. The basic idea is to estimate supercapacitor parameters in real time based on an online algorithm and measurements of current and voltage. In [16], Chaoui *et al.* proposed an online capacitance estimation algorithm for supercapacitors based on an adaptive observer, and its stability has been proved with the Lyapunov method. A sliding mode observer is designed in [17] to estimate the capacitance and ESR of supercapacitors, where the capacitance is assumed to vary with bias voltage. In [18], a procedure integrating fuzzy logic and neural network is proposed to estimate supercapacitors' ESR and capacitance. Soualhi *et al.* [19] proposed an extended Kalman filter to estimate the capacitance and ESR of supercapacitors, where the supercapacitor model is considered as a noisy nonlinear model. In [20], an RLS algorithm is proposed to estimate the ESR and capacitance of supercapacitors, and then the model parameters are used to estimate the state-of-energy of the cell.

Motivated by these works, in this paper, we propose an SoH-aware energy-efficient charging algorithm by estimating the cell capacitance and balancing resistance in real time. The capacitance and balancing resistance are estimated using an RLS algorithm developed in [20]. Then the estimated parameter values instead of their nominal values are used in the charging decision computation. Both simulation and experiment results are provided to verify the superiority and effectiveness of the proposed design.

III. Preliminaries and Motivations

In this section, we first introduce the switched resistor circuit and classic charging methods for supercapacitors. We will then elaborate the limitations of existing charging methods in energy efficiency and the main idea to mitigate it.

A. Charging Circuit and Methods

In the switched resistor circuit, a balancing resistor R_k is connected in parallel with cell k through switch S_k. Assume there are N cells in the system, and the set of cells is denoted as $\mathbf{V} = \{1, 2, \cdots, N\}$. The voltage dynamics of each cell is derived as

$$C_k \cdot \frac{\mathrm{d}v_k}{\mathrm{d}t} = i_c - \frac{v_k}{R_k} \cdot d_k, \quad k \in \mathbf{V}, \tag{1}$$

where C_k, v_k, and d_k represent the capacitance, voltage, and duty cycle of cell k, respectively, the differential $\mathrm{d}v_k/\mathrm{d}t$ is also called the charging rate, i_c is the charging current from the external power source, and R_k is the resistance of the balancing resistor. R_k is normally chosen as

$$R_k = \frac{v_0}{i_c}, \tag{2}$$

where v_0 is the cell voltage upon fully charged.

Supecapacitors are usually modeled as a series resistor-capacitor (RC) circuit in high-power applications [3]. Such a circuit model can be simplified to a capacitor in portable applications, as the voltage drop of the ESR is negligible [14]. It is also worth mentioning that the capacitances of supercapacitors slightly increase with cell voltages due to the faradic current from reactions [19]. In portable applications, such a deviation can also be neglected and the capacitance is assumed to be constant [21]. The fidelity of this simplified supercapacitor model is verified experimentally in Section V-B.

A commercially available constant-current power source is chosen as the external power source. This is because: (i) constant-current charging avoids the safety concerns on large transient currents caused by its alternative, i.e., the constant-voltage charging [21]; and (ii) constant-current charging achieves fast charging by providing a steady charging current [22]. This means the charging current i_c in (2) is a constant, which in turn, indicates a constant resistance R_k.

This way, we can see that the only design parameter in Eq. (1) is the duty cycle d_k, which leads to two classic charging methods in the literature: $1-$ charging method [11] and $0-1$ charging method [12].

• **1– Charging Method**. $1-$ charging is a classic method to charge supercapacitors, with which all switches are kept

0885-8969 (c) 2018 IEEE. Personal use is permitted, but republication/redistribution requires IEEE permission. See http://www.ieee.org/publications_standards/publications/rights/index.html for more information.

This article has been accepted for publication in a future issue of this journal, but has not been fully edited. Content may change prior to final publication. Citation information: DOI 10.1109/TEC.2018.2841427, IEEE Transactions on Energy Conversion

on during charging, thus removing the necessity of balancing switches. The voltage of each cell is calculated as

$$v_k(t) = i_c R_k + [v_k(0) - i_c R]\, e^{-\frac{t}{RC_k}}, \tag{3}$$

and thus the final voltage of cells is

$$\lim_{t\to\infty} v_k(t) = i_c R_k = v_0, \tag{4}$$

implying cells can be fully charged eventually.

• **0–1 Charging Method**. Another classic charging method is the $0-1$ method: switch k is turned off (i.e., $d_k = 0$) if the cell voltage is less than the desired value v_0, and turned on (i.e., $d_k = 1$) otherwise. The cell voltage before being fully charged is derived as

$$v_k(t) = v_k(0) + \frac{i_c}{C_k} t, \quad d_k = 0. \tag{5}$$

From (1), we know that the fastest charging rate is achieved when $d_k = 0$. Then with the given circuit parameters, the minimal charging time for cell k from the initial voltage $v_k(0)$ to the desired voltage v_0 is calculated as

$$T_k = \frac{C_k\,[v_0 - v_k(0)]}{i_c}. \tag{6}$$

B. Energy Efficiency Analysis

For the switched resistor circuit, its energy efficiency hinges crucially on the charging time. The charging time for a supercapacitor module is defined as the time until all cells are fully charged. The minimal charging time T for a module is defined as the maximum of the minimal charging time of cells

$$T = \max\{T_k, k \in \mathbf{V}\}. \tag{7}$$

Thus the minimal charging time of a module is dominated by the worst cell, i.e., the last cell being fully charged.

In the $1-$ charging method, the charging time of the module is even longer than that of the worst cell since the switches are always on. The $0-1$ charging method, on the other hand, achieves the minimal charging time as cells are charged freely with $d_k = 0$ until they are fully charged. It is crucial to guarantee the minimal charging time because the prolonged charging time (i) degrades the user satisfaction seriously, and (ii) indicates a lower energy efficiency.

The energy efficiency of a charging system is defined as the ratio of the stored energy of cells to the input energy from the external power source

$$\eta = \frac{E_{st}}{E_{in}}, \tag{8}$$

where the stored energy E_{st} when cells are charged from $v_k(0)$ to v_0 is

$$E_{st} = \frac{1}{2}\sum_{k=1}^{N} C_k\big[v_0^2 - v_k^2(0)\big], \tag{9}$$

and the input energy E_{in} is

$$E_{in} = \sum_{k=1}^{N}\int_0^t v_k(\tau) i_c \mathrm{d}\tau = i_c \sum_{k=1}^{N}\int_0^t v_k(\tau)\mathrm{d}\tau, \tag{10}$$

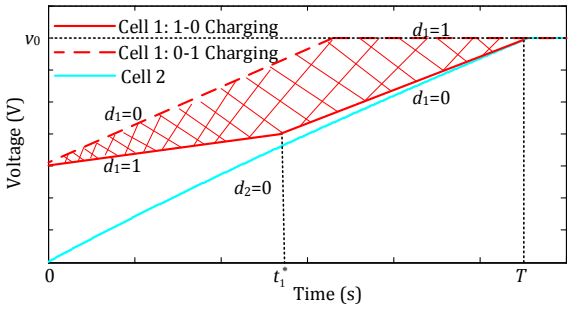

Fig. 2. The charging profile of the $1-0$ charging method for cell 1. Cell 2 is charged with $d_2 = 0$. The marked area means the saved energy compared with the $0-1$ charging method.

and t is the charging time for the module.

Recent studies have shown that the stored energy $E_k(t)$ in a cell k follows a more general expression $E_k(t) = mC_k v_k^2(t)$, where the coefficient m is determined by some factors, such as the dispersion coefficient of the cell over a wide frequency range [23], [24]. The coefficient m is equal to $1/2$ only in ideal non-dispersive storage devices [23]. However, to simplify the analysis, we assume cells are non-dispersive, which implies that $m = 1/2$. The effectiveness of such a simplification for supercapacitors has been verified in, e.g., [25], [26].

The $0-1$ charging method, albeit achieves the shortest charging time, cannot maximize the energy efficiency, implying the charging system may suffer from a considerable power loss and thermal heating, which will be illustrated in what follows.

C. How to Improve Energy Efficiency?

As explained previously, energy efficiency (i.e., Eq (8)) is defined as the ratio of the stored energy (i.e., Eq. (9)) to the input energy (i.e., Eq. (10)). The stored energy is invariant to the applied charging methods since cells are charged from the same initial voltages to the same desired voltage. Then, the only way to improve energy efficiency is to minimize the input energy from the external power source. From (10), we find that with a given charging current i_c, the input energy is dominated by the integral area encircled by the voltage curve and charging time — *we can maximize the energy efficiency by minimizing the encircled area.*

To minimize the encircled area, we first need to guarantee (i) the worst cell m is charged with duty cycle 0, and (ii) other cells $k \in \mathbf{V}, k \neq m$ are fully charged at T, where T is determined by the worst cell according to (7). Then, we can minimize the encircled area for all other cells $k \in \mathbf{V}, k \neq m$ by regulating their charging profiles. With given initial point $v_k(0)$ and terminal point $v_k(T) = v_0$, we know the encircled area of a concave charging profile is smaller than that of a convex charging profile. Thus, charging with slow rate $d_k(t_k^{*-}) = 1$ first and then with fast rate $d_k(t_k^{*+}) = 0$, i.e., $1-0$ charging, requires less input energy than the classic $0-1$ charging, where t_k^* is the switching time, as shown in Fig. 2.

In Fig. 2, the worst cell (cell 2) is charged with duty cycle $d_2 = 0$ until T and cell 1 is fully charged at T, i.e., $v_k(T) = v_0$. The red marked area is the energy saved for charging cell 1

0885-8969 (c) 2018 IEEE. Personal use is permitted, but republication/redistribution requires IEEE permission. See http://www.ieee.org/publications_standards/publications/rights/index.html for more information.

This article has been accepted for publication in a future issue of this journal, but has not been fully edited. Content may change prior to final publication. Citation information: DOI 10.1109/TEC.2018.2841427, IEEE Transactions on Energy Conversion

using the $1-0$ charging method compared with the $0-1$ charging method. The switching time of cell 1 is t_1^*. From Fig. 2, we can find that the energy efficiency is improved using this new charging method. The effectiveness of the proposed method in maximizing the energy efficiency will be proved in the following.

IV. SoH-Aware Energy-Efficient Charging

In this section, we present the SoH-aware energy-efficient charging method. We first provide a sufficient and necessary condition for the energy efficiency maximization. Then, an RLS-based SoH estimation algorithm is designed to estimate the capacitance and balancing resistance in real time. Thereafter, the SoH-aware energy-efficient charging algorithm is proposed to be implemented in micro-controllers.

A. Energy-Efficient Charging

We have argued that the $1-0$ charging method maximizes the energy efficiency. Next we prove it analytically.

Theorem 1 Assume the supercapacitor module is comprised of N cells, where the physical topology of cells is shown in Fig. 1 and the worst cell is denoted as m. The energy efficiency can be maximized within charging time T if and only if the following conditions hold:

- Cell m is charged with duty cycle $d_k = 0$ until it is fully charged;
- All the other cells $k \in \mathbf{V}, k \neq m$ are first charged with duty cycle $d_k(t_k^{*-}) = 1$ and then with $d_k(t_k^{*+}) = 0$ (i.e., $1-0$ charging), where the switching time t_k^* is given by

$$t_k^* = \left\{ t \in R_0^+ \,\middle|\, \frac{i_c}{C_k}(T-t) + [v_k(0) - i_c R_k]\, e^{-\frac{t}{R_k C_k}} = 0 \right\}, \tag{11}$$

where R_0^+ is the nonnegative real number set.

Proof. We first prove that the choice of t_k^* can guarantee the charging is finished at T. Then we prove $1-0$ charging can maximize the energy efficiency.

The worst cell m is charged with duty cycle $d_m = 0$. Then from (6) and (7), we know cell m is fully charged at $T_m = T$. For the other cells $k \in \mathbf{V}, k \neq m$ that are charged with the $1-0$ method, we compute the cell voltage at the switching time t_k^* by (3) and (5):

$$\begin{cases} v_k(t_k^*) = i_c R_k + [v_k(0) - i_c R_k]\, e^{-\frac{t_k^*}{R_k C_k}}, \\ v_0 = v_k(t_k^*) + \dfrac{i_c}{C_k}(T - t_k^*), k \in \mathbf{V}, k \neq m, \end{cases} \tag{12}$$

from which we can compute the switching time t_k^* as in (11). Thus the switching time (11) can guarantee all the other cells are fully charged at T.

It is worth noting that the choice of the switching time t_k^* in (11) is only a sufficient condition for cells to be fully charged at T. In fact, we have infinite choices to guarantee that cells can be fully charged at T. However, only the choice in (11) can maximize the energy efficiency, which will be proved in what follows.

It is straight-forward that the energy efficiency for charging cell m is maximized with $d_m = 0$; otherwise, the charging time will be prolonged and the energy efficiency will be reduced. For the other cells $k \in \mathbf{V}, k \neq m$, we divide the charging process into two stages, i.e., $[0, t_k^*)$ stage and $[t_k^*, T]$ stage.

From the analysis in Section III-C, we know that the energy efficiency is determined by the input energy (10), which is captured by the integral of the voltage curve with the charging time. For cell $k \in \mathbf{V}, k \neq m$, the initial point $v_k(0)$ and the terminal point $v_k(T) = v_0$ are fixed regardless of charging methods, and then we have the observation:

$$v_k^a(t) \leq v_k^b(t) \Rightarrow \int_0^T v_k^a(t)\mathrm{d}t \leq \int_0^T v_k^b(t)\mathrm{d}t, \quad 0 \leq t \leq T, \tag{13}$$

where $v_k^a(t), v_k^b(t) \geq 0$ represent the voltages of cell k with charging methods a and b at time instant t.

The equation (13) implies that if we can prove the cell voltage of the $1-0$ method is always the lowest during the charging process, we can prove that the input energy of the $1-0$ method is minimized, i.e., the energy efficiency is maximized.

From (1), we know that the voltage increase rate is determined by the duty cycle d_k. If $d_k = 0$, the voltage has the fastest increase rate. If $0 < d_k \leq 1$, the charging rate gets slower with the increase of voltage. If $d_k = 1$, the voltage has the slowest increase rate. With the same initial point $v_k(0)$, we have

$$v_k^{1-0}(t) \leq v_k^d(t), \quad 0 \leq t < t_k^*, \tag{14}$$

where $v_k^{1-0}(t)$, $v_k^d(t)$ are the voltages of cell k with the $1-0$ charging method, and any duty cycle $0 \leq d_k \leq 1$.

In the stage $[t_k^*, T]$, we prove the energy efficiency maximization through contradiction. If $v_k^d(t) < v_k^{1-0}(t)$ for $t_k^* \leq t \leq T$, the voltage increase rate of $v_k^d(t)$ must be larger than $v_k^{1-0}(t)$ since they have the same terminal point $v_k(T) = T_0$. However, we already know that $v_k^{1-0}(t)$ has the fastest increase rate during $t_k^* \leq t \leq T$ as the duty cycle $d_k = 0$. This implies that the duty cycle of $v_k^d(t)$ will be less than zero, which is impossible. Thus we have

$$v_k^{1-0}(t) \leq v_k^d(t), \quad t_k^* \leq t \leq T. \tag{15}$$

From (14) and (15), we know that the $1-0$ charging has the lowest voltage curve during the charging process. Then from (13), we know that the input energy of the $1-0$ charging method is minimized, i.e., the energy efficiency is maximized. This completes the proof. □

Note that i_c, $v_k(0)$, C_k, and R_k can be directly measured, and the minimal charging time T can be calculated accordingly, thus the switching time t_k^* can be calculated from (11) and implemented in micro-controllers.

B. SoH Estimation

In the implementation, parameters i_c and $v_k(0)$ are measured by the micro-controller, while the nominal values of R_k and C_k are stored in the micro-controller. Since both the cells and balancing resistors age during the long-term operation, the nominal value stored in the micro-controller at the design time will deviate from the true value, which is commonly referred

0885-8969 (c) 2018 IEEE. Personal use is permitted, but republication/redistribution requires IEEE permission. See http://www.ieee.org/publications_standards/publications/rights/index.html for more information.

This article has been accepted for publication in a future issue of this journal, but has not been fully edited. Content may change prior to final publication. Citation information: DOI 10.1109/TEC.2018.2841427, IEEE Transactions on Energy Conversion

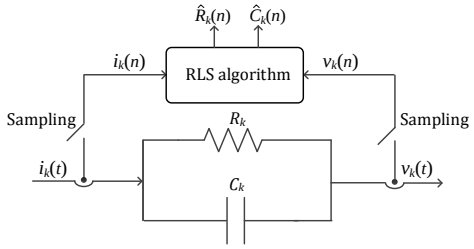

Fig. 3. The schematic of the online parameter identification for cell k.

to as the SoH degradation effect [16]. As a result, applying the switching time t_k^* computed from the inaccurate nominal values to the system will degrade the charging efficiency. To address this challenge, we develop a recursive least square (RLS) algorithm to monitor the SoH degradation and identify the capacitance and balancing resistance in real time.

In the proposed charging method, the worst cell m is charged with $d_m = 0$, and the other cells $k \in \mathbf{V}, k \neq m$ have a two-stage charging. In the first stage $[0, t_k^*)$, the cell is charged with $d_k = 1$, i.e., the equivalent circuit is a parallel RC circuit; in the second stage $[t_k^*, T]$, the cell is charged with $d_k = 0$, i.e., the equivalent circuit is a capacitor. In order to determine the switching time t_k^* accurately, we need to determine the capacitance C_k and resistance R_k during the first stage. The schematic of the online parameter identification for cell k is shown in Fig. 3.

The transfer function model of the parallel RC circuit in the first stage charging is derived as

$$\frac{V_k(s)}{I_c(s)} = \frac{R_k}{R_k C_k s + 1}, \tag{16}$$

where $V_k(s)$, $I_c(s)$ are the Laplace transforms of $v_k(t)$ and $i_c(t)$.

The z-domain transfer function of (16) is obtained as

$$\frac{V_k(z)}{I_c(z)} = \frac{R_k \mathrm{T}}{-R_k C_k z^{-1} + R_k C_k + \mathrm{T}}, \tag{17}$$

where $s = (z-1)/(\mathrm{T}z)$ and T is the sampling period of the micro-controller.

Then the discrete-time system dynamics is derived as

$$v_k(n) = -\frac{R_k C_k}{\mathrm{T}} \Delta v_k(n) + R_k i_c(n), \tag{18}$$

where $\Delta v_k(n) = v_k(n) - v_k(n-1)$.

Now, we have obtained the system dynamics (18) in the form that the RLS algorithm can be applied to. Rearranging (18) in the vector form, we have

$$v_k(n) = \zeta^T(n) \cdot \theta(n), \tag{19}$$

where

$$\begin{aligned} \zeta(n) &= \left[-\Delta v_k(n)/\mathrm{T}, i_c(n)\right]^T \\ \theta(n) &= \left[\tau_k, R_k\right]^T, \end{aligned} \tag{20}$$

and $\tau_k = R_k C_k$.

Algorithm 1 SoH-Aware EFC Algorithm

Input:

Initialize $n = 0$, $\theta(0)$, $\mathbf{P}(0)$.

Initialize λ, T, i_c, R, v_0, $v_l(0)$ and C_l for $l \in \mathbf{V}$.

Main Loop:

while $v_l(n) \leq v_0$ **do**

1: Identify cell m and compute $T(n)$ using (6) and (7). Compute $t_k^*(n)$ for cell k using (11), $\forall k \in \mathbf{V}$, $k \neq m$.
2: Charge cell m with $d_m(n) = 0$.
3: **if** $n \leq \dfrac{t_k^*(n)}{\mathrm{T}}$ **then**
4: Charge cell k with $d_k(n) = 1$.
5: Estimate $C_k(n)$ and $R(n)$ using (20) and (21), and estimate $C_m(n)$ using (21) and (22).
6: **else**
7: Charge cell k with $d_k(n) = 0$.
8: **endif**
9: $n = n + 1$.

endwhile

By applying the standard RLS algorithm, the online identification procedure is obtained as [27]:

$$\begin{aligned} \hat{\theta}(n) &= \hat{\theta}(n-1) + g(n)\left[v_k(n) - \zeta^T \hat{\theta}(n-1)\right], \\ g(n) &= \lambda^{-1}\mathbf{P}(n-1)\zeta(n)\left[1 + \lambda^{-1}\zeta^T(n)\mathbf{P}(n-1)\zeta\right]^{-1}, \\ \mathbf{P}(n) &= \lambda^{-1}\mathbf{P}(n-1) - \lambda^{-1} g(n)\zeta^T(n)\mathbf{P}(n-1), \end{aligned} \tag{21}$$

where λ is the adaptation constant, $g(n)$ is the gain vector, $\mathbf{P}(n)$ is the correlation matrix, and $\hat{\theta}(n)$ is the estimated parameter vector.

Now, with (20) and (21), we can estimate the real values of C_k and R_k through the measurement of charging current i_c and cell voltage v_k. Similarly, the parameter C_m of the worst cell m can be identified using the procedure (21), with the parameter vector and variable vector defined as

$$\begin{aligned} \zeta(n) &= \left[v_m(n-1), \mathrm{T} i_c(n)\right]^T, \\ \theta(n) &= \left[1, 1/C_m\right]^T. \end{aligned} \tag{22}$$

With the parameter identification procedures, we can estimate the real values of the parameters even if they have undergone a severe aging effect. Then, the estimated parameter values are used in the computation of switching time t_k^*. Combining the energy-efficient charging strategy in Section IV-A and the SoH estimation algorithm above, we propose the following SoH-aware energy-efficient charging algorithm.

C. SoH-Aware EFC Algorithm

We propose an online SoH-aware energy-efficiency charging (SoH-aware EFC) algorithm, as shown in Algorithm 1. The algorithm consists of three main procedures, i.e., charging indicator computation (step 1), energy-efficient charging execution (steps 2, 4, and 7), and online parameter identification (step 5). In the first procedure, the micro-controller computes the indicators T and t_k^* based on the current parameter values. Then the energy-efficient charging is conducted by comparing

0885-8969 (c) 2018 IEEE. Personal use is permitted, but republication/redistribution requires IEEE permission. See http://www.ieee.org/publications_standards/publications/rights/index.html for more information.

This article has been accepted for publication in a future issue of this journal, but has not been fully edited. Content may change prior to final publication. Citation information: DOI 10.1109/TEC.2018.2841427, IEEE Transactions on Energy Conversion

the current time slot with the switching time t_k^*. In the third procedure, the parameter values are updated by the RLS algorithm. Then the proposed charging algorithm can be operated in micro-controllers in an iterative fashion until cells are fully charged.

In the implementation of the proposed charging method, it is worth noting that the RLS algorithm does not need to work at every sampling period during the charging process. Since the capacitances and balancing resistances can be assumed as constants during the charging process, the RLS algorithm only needs to be activated at the startup stage to identify the capacitances and resistances, which are then used in the whole charging process. This implies that the computation efficiency of the proposed charging method can be further improved.

V. Performance Evaluation

In this section, we evaluate the performance of the proposed charging method using both simulation and experiment results. Without loss of generality, we consider an energy storage system with three cells. For modularity and standardization, the nominal capacitances of the three cells are set the same. But in the long-term operation, the cells suffer from the aging effects, implying that the actual capacitances may be different from the nominal value. In the proposed charging method, the system parameters are first identified using the RLS algorithm, and then the identified parameters are used in the charging control design. It is worth noting that although the evaluation is based on the three-cell case, the proposed method is general and can be applied in supercapacitor energy storage systems with $N \geq 2$ cells.

The parameters of Algorithm 1 are set as follows by default, unless otherwise specified. The nominal capacitance of three cells is $150\,\mathrm{F}$, the charging current $i_c = 2\,\mathrm{A}$, desired voltage $v_0 = 2\,\mathrm{V}$, balancing resistance $R = 1\,\Omega$, and sampling period $\mathrm{T} = 0.001\,\mathrm{s}$. The adaptation constant $\lambda = 0.92$, the parameter vector $\theta(0) = [0, 0.5]^T$, and correlation matrix [20]:

$$\mathbf{P}(0) = 10^{10} \begin{bmatrix} 1 & 0 \\ 0 & 1 \end{bmatrix}.$$

A. Simulation Evaluation

1) Simulation Setup: Consider the cells undergo a severe aging effect after the long-term operation, where capacitances of cell 1, cell 2, and cell 3 are assumed to have a 5%, 15% and 20% degradation of the nominal value, and the resistors R_1 and R_2 are assumed to have a 2% and 3% increase from the nominal value, respectively. This means that the actual values of the capacitances are $C_1 = 142.5\,\mathrm{F}$, $C_2 = 127.5\,\mathrm{F}$, $C_3 = 120\,\mathrm{F}$, and the actual resistances of the balancing resistors are $R_1 = 1.02\,\Omega$ and $R_2 = 1.03\,\Omega$. The simulations are conducted in Matlab/Simulink.

The actual values of the system parameters can be estimated online using the RLS algorithm through the current and voltage measurements in the charging process. The parameter identification for the three cells is shown in Fig. 4, where we find the estimations of the capacitances of cell 1, cell 2 and cell 3 converge to $142.5\,\mathrm{F}$, $127.5\,\mathrm{F}$, and $120\,\mathrm{F}$, respectively, which are the same as their actual values. Moreover, the

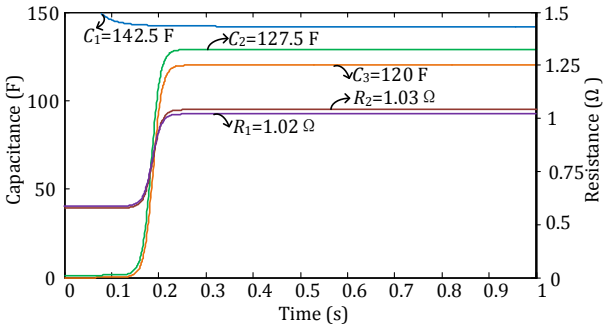

Fig. 4. The parameter identification for three cells in the simulation setup.

estimations of the resistances of R_1 and R_2 also converge to their actual values $R_1 = 1.02\,\Omega$ and $R_2 = 1.03\,\Omega$, respectively. The convergence time of the parameter identification is less than $0.3\,\mathrm{s}$, which implies that the RLS algorithm can be only activated at the startup stage of the charging process. In the simulation setup, we assume cells suffer from uneven SoH degradations and have different capacitances, and then the initial voltages of the cells are typically different in the repeated charging-discharging processes [13]. To emulate the phenomena, we set the initial voltages of the cells are $v_1(0) = 1.2\,\mathrm{V}$, $v_2(0) = 0.9\,\mathrm{V}$, and $v_3(0) = 0.6\,\mathrm{V}$. From (6) and (7), we know cell 3 is the worst cell and R_3 is not connected into the circuit, and thus the resistance of R_3 is not estimated in the parameter identification process.

2) Simulation Results: We evaluate the effectiveness of the proposed charging method with simulation results. The proposed SoH-aware EFC method is compared with its counterpart, i.e., SoH-unaware EFC method, where the charging decisions are computed using the nominal values instead of the actual values of the capacitances and resistances. The charging profiles of the SoH-unaware EFC method and SoH-aware EFC method are shown in Fig. 5. Fig. 5(a) depicts the charging profile of the SoH-unaware EFC method, where the calculation of switching times is based on the nominal values of system parameters. Based on (11), the switching times are computed as $t_1^* = 43\,\mathrm{s}$ and $t_2^* = 67\,\mathrm{s}$. From Fig. 5(a), we find the charging time of the three cells is $103\,\mathrm{s}$. Based on (9) and the charging profiles in Fig. 5(a), the energy efficiency is computed as 76%. Fig. 5(b) shows the charging profile of the SoH-aware EFC method, where cells can identify the actual values of system parameters in real time. Then the actual values of the system parameters are used in the computation of the switching time $t_1^* = 27.5\,\mathrm{s}$ and $t_2^* = 41\,\mathrm{s}$, respectively. The charging time of the three cells is $84\,\mathrm{s}$, and the energy efficiency during the charging process is computed as 86.2%.

From the simulation results, it can be found that the SoH-aware EFC method can monitor the SoH degradation of cells and estimate the actual values of the system parameters in real time. However, the SoH-unaware EFC method cannot react to the SoH degradation of cells, which implies the charging decision computation is directly based on the inaccurate nominal values, resulting in the decrease of the energy efficiency and the prolonging of the charging time. The simulation results of Fig. 5 are summarized in Table I, where we can

0885-8969 (c) 2018 IEEE. Personal use is permitted, but republication/redistribution requires IEEE permission. See http://www.ieee.org/publications_standards/publications/rights/index.html for more information.

This article has been accepted for publication in a future issue of this journal, but has not been fully edited. Content may change prior to final publication. Citation information: DOI 10.1109/TEC.2018.2841427, IEEE Transactions on Energy Conversion

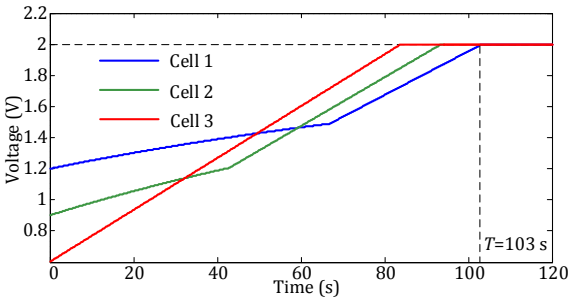

(a) SoH-unaware EFC

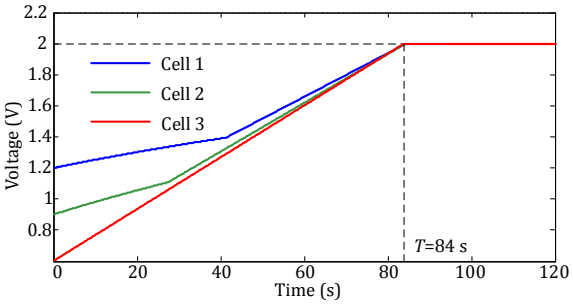

(b) SoH-aware EFC

Fig. 5. Simulation comparisons of the SoH-unaware EFC method with the proposed SoH-aware EFC method.

find that, compared with the SoH-unaware EFC method, the performance of the SoH-aware EFC method is significantly improved when SoH degradations occur.

TABLE I
SUMMARY OF SIMULATION RESULTS IN FIG. 5

Metric\Method	SoH-unaware EFC	SoH-aware EFC
Charging time (s)	103	84
Energy Efficiency	77.6%	86.2%

B. Experiment Evaluation

1) Experiment Setup: Fig. 6 depicts the hardware setup of the supercapacitor charging testbed, which is built based on the schematic of Fig. 1. The testbed consists of a main board, three supercapacitor cells, three resistors, a DC 24 V power source, a constant-current power source, a measurement board, a PXI platform, and the Labview in a hosting computer. The main board is comprised of a DSP TMS320F2808 micro-controller, three IRF530 MOSFETs working as switches, a current sensor CSM005A, three high-precision dividers working as voltage sensors, and a voltage conversion chip PDUKE-24S05.

The 2808 controller measures the output voltage of each cell of type Maxwell BCAP0150P270T07 through the high-precision voltage divider, and measures the charging current through the current sensor CSM005A with a measurement range of 0–10 A. With the measurements, the 2808 controller computes the duty cycles based on the programmed algorithm. Then, the duty cycles are used to generate PWM signals to regulate the switches IRF530 MOSFETs through the PWM optocoupler/driver TLP700A. The 2808 controller,

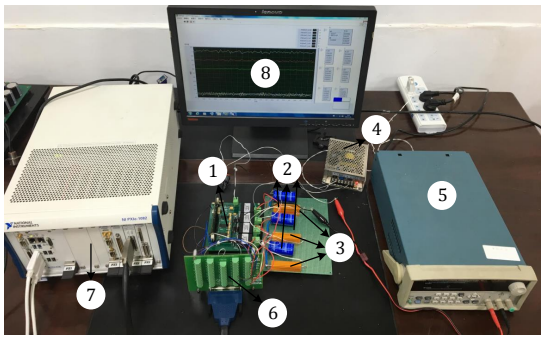

Fig. 6. The experiment setup. (1) main board; (2) three supercapacitor cells; (3) three resistors; (4) DC 24 V power source; (5) constant-current power source; (6) measurement board; (7) PXI platform; (8) Labview.

which provides 16 PWM outputs and 16-bit ADCs, has been programmed and debugged with the Code Composer Studio (CCS) in the hosting desktop.

The DC 24 V power source supplies operating voltages for the micro-controllers and sensors through the voltage conversion chip PDUKE-24S05. The constant-current power source supplies the charging current for the three cells. The PXI platform collects the output of the system through the measurement board, and displays the signals with Labview in the hosting desktop.

PXI is a rugged PC-based platform for measurement and automation systems. PXI is an open industry standard governed by the PXI Systems Alliance to promote the PXI standard, ensure interoperability, and maintain the PXI specification. PXI has been proved a high-performance and low-cost deployment platform for applications such as manufacturing test, machine monitoring, automotive, and industrial test [28].

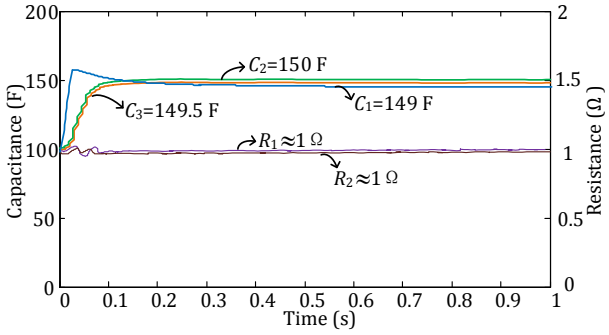

Fig. 7. The parameter identification for three cells in the experiment setup.

In the long-term operation, the capacitances and resistances may deviate from their nominal values at the design time. Thus, it is necessary to identify the system parameters at the startup stage of the charging process. Fig. 7 shows the parameter identification for the three cells in the experiment setup. In the RLS algorithm, the initial values of the capacitances and resistances are chosen as $C_k(0) = 100\,\text{F}$, and $R_k(0) = 1\,\Omega$, respectively. From Fig. 7, we find that the estimated values of the capacitances $C_1 = 149\,\text{F}$, $C_2 = 150\,\text{F}$, and $C_3 = 149.5\,\text{F}$, which are very close to the nominal value 150 F. Moreover, the estimations of R_1 and R_2 can be also considered approximately the same as the nominal

0885-8969 (c) 2018 IEEE. Personal use is permitted, but republication/redistribution requires IEEE permission. See http://www.ieee.org/publications_standards/publications/rights/index.html for more information.

This article has been accepted for publication in a future issue of this journal, but has not been fully edited. Content may change prior to final publication. Citation information: DOI 10.1109/TEC.2018.2841427, IEEE Transactions on Energy Conversion

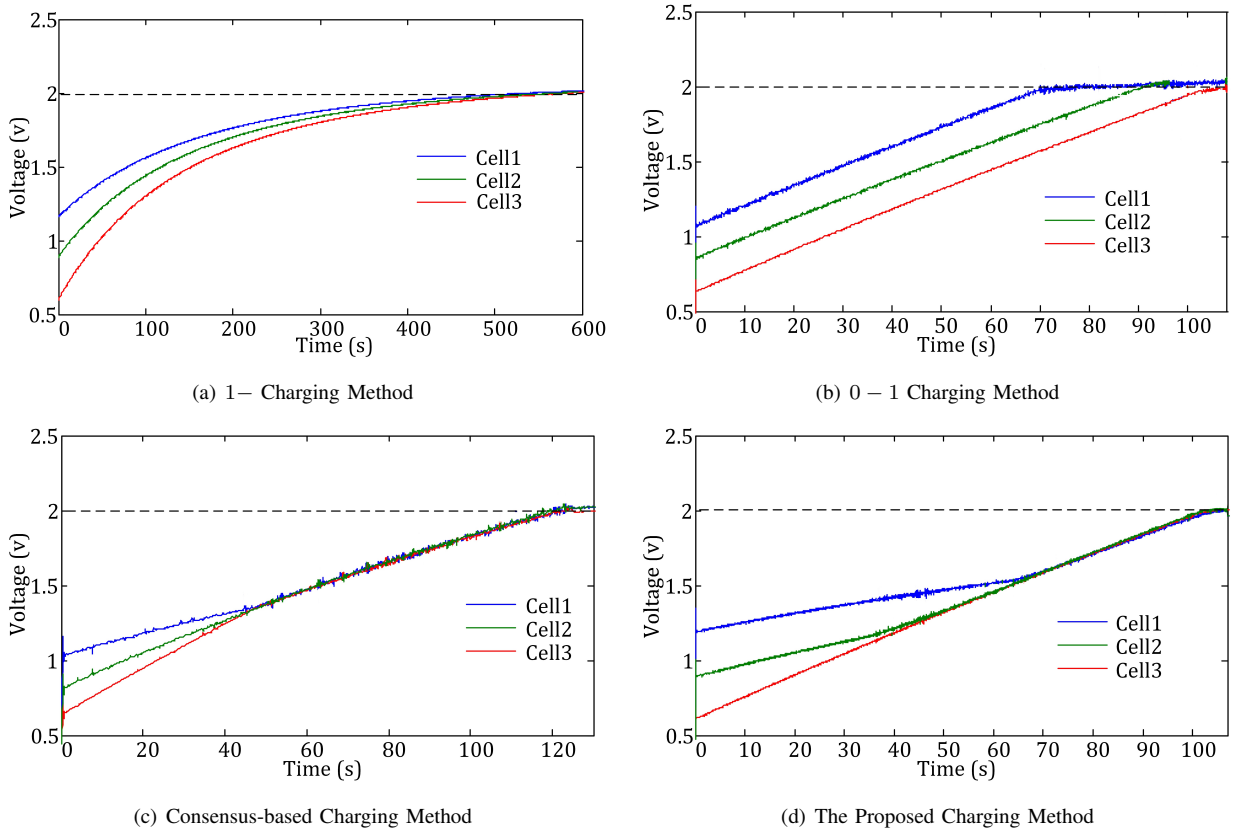

(a) $1-$ Charging Method

(b) $0-1$ Charging Method

(c) Consensus-based Charging Method

(d) The Proposed Charging Method

Fig. 8. Experimental comparisons of the proposed charging method with existing charging methods.

value $1\,\Omega$. This is because the prototype is rather new, where the cells and resistors have not undergone the sufficient aging effect. However, to evaluate the performance of the proposed charging method with uneven SoH degradations, we set the initial voltages of three cells differently as $v_1(0) = 1.2\,\text{V}$, $v_2(0) = 0.9\,\text{V}$, and $v_3(0) = 0.6\,\text{V}$. Similar to the simulation setup, cell 3 is the worst cell and R_3 is not connected into the circuit, and thus the resistance of R_3 is not estimated in the parameter identification process.

2) Experiment Results: The charging profiles of different charging methods are shown in Fig. 8. Fig. 8(a) depicts the charging profile of the $1-$ charging method, where the charging time is about 600 s and the energy efficiency is 11.3%. The charging time is determined by the time that all cells are fully charged and the energy efficiency is computed based on the charging profile and (8). We can find that the charging time is very long and the energy efficiency is relatively low. The charging profile of the $0-1$ charging method is shown in Fig. 8(b), where the charging time is about 105 s and the energy efficiency is 73.5%. The charging time is determined by the worst cell, i.e., cell 3. Fig. 8(c) shows the charging profile of the average consensus-based method, where the charging time is about 120 s and the energy efficiency is 67.5%. Compared with the $0-1$ method, the average consensus-based method prolongs the charging time and reduces the energy efficiency. Fig. 8(d) shows the charging profile of the proposed method with the charging time of 105 s and the energy efficiency of 81%. Compared with the $0-1$ method, the proposed method improves the energy efficiency with the same charging time. It is shown that the three cells reach the desired voltage at $T = 105\,\text{s}$ simultaneously. Moreover, the switching time $t_1^* = 43\,\text{s}$ and $t_2^* = 67\,\text{s}$ are almost the same as theoretical results $t_1^* = 43.1\,\text{s}$ and $t_2^* = 66.7\,\text{s}$ obtained from (11). This fact implies the cell models (3) and (5) have a good fidelity.

From the experiment results, we find that the proposed charging method and the $1-0$ method have the minimal charging time, while the charging time of the $1-$ method and the consensus-based method is significantly prolonged. This is because that, in the proposed method and the $1-0$ method, the charging time is dominated by the worst cell (cell 3), which is charged with the fastest rate ($d_3 = 0$) before it is fully charged. However, in the $1-$ method and the consensus-based method, the duty cycle of the worst cell (cell 3) is not always 0, which prolongs the charging time. The prolonged charging time implies more energy will be consumed on resistors, which reduces the energy efficiency of the system during the charging process. Compared with the $1-0$ method, the proposed method further improves the energy efficiency by maintaining low charging profiles of cell 1 and cell 2. The experiment results of Fig. 8 are summarized in Table II. We can find that the proposed method considerably improves the energy efficiency with the minimal charging time.

C. Results Discussion

The performance evaluation of the proposed charging method is summarized as follows.

0885-8969 (c) 2018 IEEE. Personal use is permitted, but republication/redistribution requires IEEE permission. See http://www.ieee.org/publications_standards/publications/rights/index.html for more information.

This article has been accepted for publication in a future issue of this journal, but has not been fully edited. Content may change prior to final publication. Citation information: DOI 10.1109/TEC.2018.2841427, IEEE Transactions on Energy Conversion

TABLE II
SUMMARY OF EXPERIMENT RESULTS IN FIG. 8

Metric\Method	$1-$	$0-1$	Consensus	Proposed
Charging time (s)	600	105	120	105
Energy Efficiency	11.3%	73.5%	67.5%	81%

1) Superiority: As shown in Table II, the energy efficiency of the proposed charging method is considerably improved compared with existing charging methods. This is because that, as depicted in Fig. 8(d), the voltage curves of the proposed charging method were maintained low profiles to minimize the input energy during the charging process. With the same stored energy, the energy efficiency of the EFC method is then maximized. If there are no SoH degradations and cells have the same parameters, both the proposed $1-0$ method and the classical $0-1$ method can maximize the energy efficiency by charging cells with duty cycles of zero. However, due to the manufacturing limitations and operating conditions, cells typically suffer from uneven SoH degradations. Then the proposed charging method shows its superiority in improving the energy efficiency by maintaining low charging profiles of cells.

2) Effectiveness: In the proposed charging method, the actual values of the system parameters are estimated online using the RLS algorithm. Then, the estimated parameter values are used in the charging decision computation, which guarantees the energy efficiency maximization based on Theorem 1 during the charging process. In the discharging process of cells, however, the most efficient method is to discharge cells with duty cycles of zero. The discharging process can be terminated when the cell with the lowest voltage reaches the voltage threshold to prevent the cells from over-discharging.

3) Practicality: The proposed charging method is suitable for low-power systems which are sensitive to charging efficiency and charging time, such as portable electronics. The proposed charging method can maximize the energy efficiency during the charging process, which will minimize the power loss on the resistors. This fact implies that the thermal heating and the temperature rise of the hardware can be alleviated. Moreover, compared with the existing methods, the proposed charging method can achieve the minimal charging time, which is important for increasing the user satisfaction with portable electronics.

VI. CONCLUSION

In this paper, we proposed a new SoH-aware energy-efficient charging method for supercapacitors with the aim of maximizing the energy efficiency during the charging process. A sufficient and necessary condition for the energy efficiency maximization is provided. The recursive-least-square algorithm is employed to estimate the SoH of cells and resistors in real time. An online SoH-aware energy-efficient charging algorithm is further proposed. Both simulation and experiment results are provided to verify the superiority and effectiveness of the proposed strategy. The practicality of the proposed method is also discussed. In the future work, we will further consider the supercapacitor charging problem with the optimal charging current profile.

REFERENCES

[1] Y. Zhang, Z. Wei, H. Li, L. Cai, J. Pan, "Optimal charging scheduling for catenary-free trams in public transportation systems," *IEEE Trans. Smart Grid*, to be published.

[2] X. Chang, Y. Li, X. Li, X. Chen, "An active damping method based on a supercapacitor energy storage system to overcome the destabilizing effect of instantaneous constant power loads in DC microgrids," *IEEE Trans. Energy Convers.*, vol. 32, no. 1, pp. 36–47, Sep. 2017.

[3] H. Li, J. Peng, J. He, R. Zhou, Z. Huang, J. Pan, "A cooperative charging protocol for onboard supercapacitors of catenary-free trams," *IEEE Trans. Control Syst. Technol.*, to be published.

[4] F. Deng, H. Qiu, J. Chen, L. Wang, B. Wang, "Wearable thermoelectric power generators combined with flexible supercapacitor for low-power human diagnosis devices," *IEEE Trans. Ind. Electron.*, vol. 64, no. 2, pp. 1477–1485, Sep. 2017.

[5] C. Shen, S. Xu, Y. Xie, M. Sanghadasa, X. Wang, L. Lin, "A review of on-chip micro supercapacitors for integrated self-powering systems," *J. Microelectromech. Syst.*, vol. 26, no. 5, pp. 949–965, Jul. 2017.

[6] D. Johnson, "Zap&go's graphene supercapacitor powers portable charger," *IEEE Spectr.*, Feb, 2016.

[7] D. Linzen, S. Buller, E. Karden, R. W. De Doncker, "Analysis and evaluation of charge-balancing circuits on performance, reliability, and lifetime of supercapacitor systems," *IEEE Trans. Ind. Appl.*, vol. 41, no. 5, pp. 1135–1141, Sep. 2005.

[8] L. Li, Z. Huang, H. Li, J. Peng, "A rapid cell voltage balancing scheme for supercapacitor based energy storage systems for urban rail vehicles," *Electr. Power Syst. Res.*, vol. 142, pp. 329–340, Jan. 2017.

[9] D. Sun, F. Wu, L. Sun, Y. Zhang, "Research on super capacitor voltage balancing of electric vehicle charging stations," *Proc. IEEE Veh. Power Prop. Conf.*, pp. 1–5, 2015.

[10] P. Kreczanik, T. Kovaltchouk, A. Hijazi, P. Venet, G. Clerc, "Consideration of the ageing in the control of the balancing circuit of supercapacitor," *Proc. Eur. Symp. Super Capacitors Appl.*, pp. 1–5, 2010.

[11] W. Ma, "Voltage equalization in super capacitors series," in *Mech. Autom. Control Syst.*, Springer, pp. 401–410, Oct. 2014.

[12] S. Lambert, V. Pickert, J. Holden, W. Li, X. He, "Overview of supercapacitor voltage equalisation circuits for an electric vehicle charging application," *Proc. IEEE Veh. Power Prop. Conf.*, pp. 1–7, 2010.

[13] S. Shili, A. Hijazi, A. Sari, X. Lin-Shi, P. Venet, "Balancing circuit new control for supercapacitor storage system lifetime maximization," *IEEE Trans. Power Electron.*, vol. 32, no. 6, pp. 4939–4948, Aug. 2017.

[14] H. Li, J. Peng, J. He, Z. Huang, J. Pan, "Synchronized cell balancing of supercapacitors," *Proc. IFAC World Congr.*, pp. 3338–3343, 2017.

[15] N. Reichbach, M. Mellincovsky, M. Peretz, A. Kuperman, "Long-term wide-temperature supercapacitor ragone plot based on manufacturer datasheet," *IEEE Trans. Energy Convers.*, vol. 31, no. 1, pp. 404–406, Sep. 2016.

[16] H. Chaoui, A. El Mejdoubi, A. Oukaour, H. Gualous, "Online system identification for lifetime diagnostic of supercapacitors with guaranteed stability," *IEEE Trans. Control Syst. Technol.*, vol. 24, no. 6, pp. 2094–2102, Feb. 2016.

[17] A. El Mejdoubi, H. Chaoui, H. Gualous, J. Sabor, "Online parameter identification for supercapacitor state-of-health diagnosis for vehicular applications," *IEEE Trans. Power Electron.*, vol. 32, no. 12, pp. 9355–9363, Jan. 2017.

[18] A. Soualhi, M. Makdessi, R. German, F. Rivas, H. Razik, S. Ali, P. Venet, G. Clerc, "Health monitoring of capacitors and supercapacitors using neo fuzzy neural approach," *IEEE Trans. Ind. Informat.*, vol. 14, no. 1, pp. 24–34, May 2017.

[19] A. El Mejdoubi, A. Oukaour, H. Chaoui, Y. Slamani, J. Sabor, H. Gualous, "Online supercapacitor diagnosis for electric vehicle applications," *IEEE Trans. Veh. Technol.*, vol. 65, no. 6, pp. 4241–4252, Sep. 2016.

[20] N. Reichbach, A. Kuperman, "Recursive-least-squares-based real-time estimation of supercapacitor parameters," *IEEE Trans. Energy Convers.*, vol. 31, no. 2, pp. 810–812, Feb. 2016.

[21] N. Devillers, S. Jemei, M.-C. Péra, D. Bienaimé, F. Gustin, "Review of characterization methods for supercapacitor modelling," *J. Power Sources*, vol. 246, pp. 596–608, Jan. 2014.

[22] Y. Parvini, A. Vahidi, S. A. Fayazi, "Heuristic versus optimal charging of supercapacitors, lithium-ion, and lead-acid batteries: An efficiency point of view," *IEEE Trans. Control Syst. Technol.*, vol. 26, no. 1, pp. 167–180, Jan. 2018.

0885-8969 (c) 2018 IEEE. Personal use is permitted, but republication/redistribution requires IEEE permission. See http://www.ieee.org/publications_standards/publications/rights/index.html for more information.

This article has been accepted for publication in a future issue of this journal, but has not been fully edited. Content may change prior to final publication. Citation information: DOI 10.1109/TEC.2018.2841427, IEEE Transactions on Energy Conversion

[23] M. E. Fouda, A. S. Elwakil, A. G. Radwan, A. Allagui, "Power and energy analysis of fractional-order electrical energy storage devices," *Energy*, vol. 111, pp. 785–792, Jun. 2016.
[24] R. Kopka, "Estimation of supercapacitor energy storage based on fractional differential equations," *Nanoscale Res. Lett.*, vol. 12, no. 1, pp. 636–646, Dec. 2017.
[25] F. M. Ibanez, "Analyzing the need for a balancing system in supercapacitor energy storage systems," *IEEE Trans. Power Electron.*, vol. 33, no. 3, pp. 2162–2171, Apr. 2018.
[26] R. Chai, Y. Zhang, "A practical supercapacitor model for power management in wireless sensor nodes," *IEEE Trans. Power Electron.*, vol. 30, no. 12, pp. 6720–6730, Dec. 2015.
[27] P. C. Young, *Recursive Estimation and Time-Series Analysis: An Introduction*. NewYork, USA: Springer, 2012.
[28] "What is PXI?" [Online]. Available: http://www.ni.com/pxi/whatis/.

Heng Li (M'17) is currently an Assistant Professor in School of Information Science and Engineering, Central South University, China. He received his Bachelor's degree and PhD degree from Central South University in 2011 and 2017, respectively. From Nov 2015 to Nov 2017, he worked as a research assistant in Department of Computer Science, University of Victoria, Victoria, Canada. His current research interests include cooperative control and energy storage systems. He is a member of IEEE.

Jun Peng (M'08) is a Professor in School of Information Science and Engineering at the Central South of University, China. She received her B.S. degree from Xiangtan University and the MSc degree from National University of Defense Technology, China, in 1987 and 1990, respectively. She received her PhD degree from Central South University in 2005. In April 1990, she joined the staff of Central South University. From 2006 to 2007, she was with School of Electrical and Computer Science of University of Central Florida, USA, as a visiting scholar. Her research interests include cooperative control; cloud computing and wireless communications.

Yanhui Zhou is currently a PhD student in the School of Information Science and Engineering, Central South University, Changsha, China. He received his Master's degree in the School of Information Science and Engineering, Central South University in 2014, and his Bachelors degree in School of Information and Electrical Engineering, Hunan University of Science and Technology, Xiangtan, China, in 2010. His current research interests include energy storage and hybrid energy management.

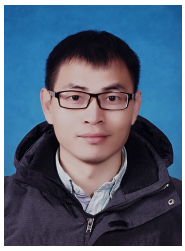

Jianping He (M'15) is currently an Associate Professor in the Department of Automation at Shanghai Jiao Tong University, Shanghai, China. He received the Ph.D. degree in control science and engineering from Zhejiang University, Hangzhou, China, in 2013, and had been a research fellow in the Department of Electrical and Computer Engineering at the University of Victoria, Canada, from Dec. 2013 to Mar. 2017. His research interests mainly include the smart sensing and control, security and privacy theory and applications, distributed learning and big data. He serves as an associate editor for the KSII Transactions on Internet and Information Systems. He was also a guest editor for the International Journal of Robust and Nonlinear Control and Neurocomputing. He received the best paper award of IEEE WCSP'17 and the finalist best student paper award of IEEE ICCA'17.

Zhiwu Huang (M'08) is a Professor in School of Information Science and Engineering at the Central South of University, China. He received his BS degree in Industrial Automation from Xiangtan University in 1987, received his MS degree in Industrial Automation from Department of Automatic Control, University of Science and Technology Beijing in 1989 and received his PhD degree in Control Theory and Control Engineering from Central South University in 2006. In October 1994, he joined the staff of Central South University. From 2008 to 2009, he was with School of Computer Science and Electronic Engineering of University of Essex, U.K., as a visiting scholar. His research interests include fault diagnostic technique and cooperative control. He is a member of IEEE.

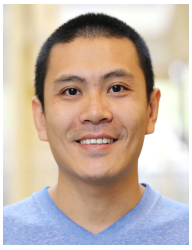

Liang He (S'09-M'12-SM'17) is an Assistant Professor with the University of Colorado Denver. He worked as a research fellow at the University of Michigan, Ann Arbor, during 2015-2017, as a research scientist with the Singapore University of Technology & Design during 2012-2014, and as a research assistant with the University of Victoria during 2009-2011. His research interests include CPSes, cognitive battery management, and networking. He has been a recipient of the best paper/poster awards of MobiSys17, QShine14, WCSP11, and GLOBECOM11, and a best paper candidate of GLOBECOM14. He is a senior member of the IEEE.

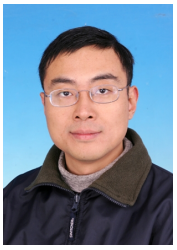

Jianping Pan (S'96-M'98-SM'08) is currently a Professor of computer science at the University of Victoria, Victoria, British Columbia, Canada. He received his Bachelors and PhD degrees in computer science from Southeast University, Nanjing, Jiangsu, China, and he did his postdoctoral research at the University of Waterloo, Waterloo, Ontario, Canada. He also worked at Fujitsu Labs and NTT Labs. His area of specialization is computer networks and distributed systems, and his current research interests include protocols for advanced networking, performance analysis of networked systems, and applied network security. He received the IEICE Best Paper Award in 2009, the Telecommunications Advancement Foundations Telesys Award in 2010, the WCSP 2011 Best Paper Award, the IEEE Globecom 2011 Best Paper Award, the JSPS Invitation Fellowship in 2012, and the IEEE ICC 2013 Best Paper Award. He is a senior member of the ACM and a senior member of the IEEE.

0885-8969 (c) 2018 IEEE. Personal use is permitted, but republication/redistribution requires IEEE permission. See http://www.ieee.org/publications_standards/publications/rights/index.html for more information.